

Power-Efficient Multi-Beam Phase-Attached Radar/Communications

Cenk Sahin*, Patrick M. McCormick*, Justin G. Metcalf[†], and Shannon D. Blunt[‡]

*Sensors Directorate, Air Force Research Laboratory, Wright-Patterson Air Force Base, OH

[†]School of Electrical and Computer Engineering, Advanced Radar Research Center, University of Oklahoma, Norman, OK

[‡]Department of Electrical Engineering & Computer Science, University of Kansas, Lawrence, KS

Abstract—Multi-function waveforms possessing simultaneous radar and communication capabilities provide the means with which to efficiently combat congestion of the spectrum. Here a joint coding/spatial diversity radar/communication waveform design approach is introduced for use with digital antenna arrays. The proposed approach combines the recently developed phase-attached radar/communication (PARC) approach with the far-field radiated emission design (FFRED) formulation to realize the transmission of multiple independent data streams in arbitrary spatial directions concurrently with active radar sensing that is minimally impacted. The resulting physical signals emitted from the elements of the multiple-input multiple-output (MIMO) array have a desirable structure that is constant-modulus and have improved spectral containment relative to the original FFRED formulation.

Index Terms—dual-function radar/communication, spectrum sharing, waveform design, waveform diversity, MIMO

I. INTRODUCTION

The loss of spectrum to commercial entities combined with increasing requirements for defense communication networks continues to reduce the available spectrum for radar systems [1]. As a result, it will become increasingly difficult to ensure successful operation of radar systems using the traditional single-function, fixed-band spectrum allocation framework. To combat growing spectral congestion while enabling successful operation of both radar and communication systems, a great deal of recent research has been dedicated to developing new techniques and paradigms to share spectrum between radar and communications functions [2]. Spectrum sharing approaches can be roughly divided into two categories [3]: co-existence approaches that focus on managing or reducing the cross-function interference from separate radar and communication systems (e.g. [4]–[6]), and co-design approaches that strive to improve the efficiency of spectral usage by developing dual-function systems having both radar and communication capabilities [7]–[16]. Here we specifically focus on the co-design problem.

Dual-function system design requires the use of some manner of waveform diversity [17], such as temporal [18], spectral [14], spatial [7], [10], [12], [13], [18] or coding diversity [8], [9], [11], [16]. Of course, temporal sharing further exacerbates an already difficult resource management problem by reducing the available time for radar operation to an unacceptable level.

Traditional spatial diversity techniques such as sub-arraying reduce the achievable spatial gain and angular resolution of the individual transmit beams [18]. Such techniques also must

be carefully considered so that spatial sidelobes of the sub-arrays do not interfere with one another. In contrast, here a new combination of coding and spatial diversity is considered as a means to improve spectral efficiency while imposing minimal degradation to radar functionality.

To achieve a coding diversity form of joint radar/communications the radar emission is varied on a pulse-to-pulse basis as a function of the communication sequence, with the set of all radar emissions thereby forming a communication alphabet. However, doing so also incurs range sidelobe modulation (RSM) of clutter [8], [19], which reduces target detection performance due to increased residual interference after clutter cancellation. That said, the phase-attached radar communication (PARC) approach [11] was recently introduced to control the impact of RSM on radar performance through the use of several tunable parameters. In addition, PARC waveforms have an FM structure, which is constant-modulus and continuous-phase, thereby ensuring both power and spectral efficiency.

Spectrum sharing via spatial diversity involves the use of an antenna array to transmit radar and communication signals simultaneously in distinct spatial directions. To preserve radar performance and due to the substantial differences between one-way and two-way path losses, the communication signal is typically emitted at a lower power via the sidelobe region [12], [13]. Far-field radiated emission design (FFRED) [12] is a general spatial diversity waveform design approach that realizes a (correlated) physical MIMO emission that has been demonstrated experimentally [20]. The FFRED approach also constrains the emitted waveforms to be constant-modulus, which results in a minimal loss in mainlobe (radar) transmit power. These constant-modulus waveforms are designed such that they combine in arbitrary desired spatial directions to form the intended radar and communication signals. Moreover, FFRED enables data rates on the order of the time-bandwidth product multiplied by the pulse repetition frequency (PRF) without compromising the radar timeline.

It is important to note that PARC was devised as a means to incorporate communications into the radar mainbeam while FFRED generates separate radar and communication beams. In addition, in some cases FFRED emissions can cause spectral spreading relative to the baseline radar-only signal. Here we combine the PARC and FFRED approaches to form a joint coding/spatial diversity MIMO waveform design that is able to transmit data in multiple spatial directions simulta-

neously, including the radar main beam, with limited impact on radar performance. Furthermore, the PARC structure limits the spectral spreading that can otherwise occur with FFRED waveforms.

II. PHASE-ATTACHED RADAR/COMMUNICATIONS (PARC)

The tunable continuous phase modulation (CPM) based PARC waveform design of [11] is a radar-embedded communication (REC) approach in which information sequences are modulated using CPM and phase-attached to a fixed (i.e. unchanging from pulse-to-pulse) polyphase-coded frequency modulated (PCFM) radar waveform [21]. The combined waveform retains the CPM structure and therefore preserves the well-known advantages of constant envelope and continuous phase. These characteristics translate to unit peak-to-average power ratio (PAPR) and good spectral containment, respectively, which ensures compatibility with high-power amplifiers required for most radar applications. In addition, the tunable parameters of PARC enable direct control of the degree of RSM by trading off communication performance (i.e. bit error rate (BER) and data throughput) [11].

The PARC waveform, constructed around a fixed radar waveform and for an arbitrary pulse repetition interval (PRI), is given as

$$\begin{aligned} s(t; \bar{\beta}, \alpha, h, T_s) &= \exp \{ j (\psi(t; \bar{\beta}) + \phi(t; \alpha, h, T_s)) \} \quad (1) \\ &= \underbrace{\exp \{ j \psi(t; \bar{\beta}) \}}_{s_r(t; \bar{\beta})} \underbrace{\exp \{ j \phi(t; \alpha, h, T_s) \}}_{s_c(t; \alpha, h, T_s)}, \end{aligned}$$

where $s_r(t; \bar{\beta})$ is the PCFM waveform implementation of the *fixed* radar code $\bar{\beta} = [\bar{\beta}_0, \dots, \bar{\beta}_{K-1}]$, with $|\bar{\beta}_k| \leq \pi$ for all $k=0, \dots, K-1$ and with K closely approximating the radar time-bandwidth product (based on 3-dB bandwidth). Likewise, $s_c(t; \alpha, h, T_s)$ is the CPM waveform resulting from modulating the 2^m -ary communication sequence $\alpha = [\alpha_0, \dots, \alpha_{N_s-1}]$, with symbol interval T_s and modulation index h , where $\alpha_{n_s} \in \{\pm 1, \pm 3, \dots, \pm(2^m - 1)\}$ for $n_s = 0, \dots, N_s - 1$ and m the *modulation order* [22]. Unlike the base radar waveform $s_r(t; \bar{\beta})$, the communication component $s_c(t; \alpha, h, T_s)$ changes on a pulse-to-pulse basis as a new communication sequence is transmitted in each pulse. The number of symbols per pulse N_s is on the order of the time-bandwidth product K ; therefore, the data rate (in bits/s) is on the order of $K \times \text{PRF}$. The communication component has the same duration as the base radar waveform (pulsewidth T), and thus the number of symbols per pulse satisfies $N_s = \frac{T}{T_s}$. The modulation index h is a key parameter that controls the total phase change due to a communication symbol transmission; the phase change due to α_{n_s} is $h\pi\alpha_{n_s}$, which occurs over the symbol interval T_s . The data transmitted in each coherent processing interval (CPI) are intended for a communication receiver located within the mainbeam of the emission¹. As

¹The communication receiver is not required to be in the region illuminated by the radar mainbeam. However, since the emitted power has its maximum value in the radar mainbeam, it is fair to assume that the communication receiver is within the radar mainbeam.

such, communication coverage (i.e. radar mainbeam only) is the primary limitation with the PARC approach.

The main challenge with coding diversity approaches such as PARC is the RSM effect [8], [19] that arises because the pulse compression of different REC waveforms leads to different range sidelobe structures. When Doppler processing is performed across the CPI of different pulse compression responses, the presence of RSM leads to increased residual clutter after cancellation, thereby degrading target detection performance. The impact of RSM can be mitigated by either increasing the coherence across the range sidelobe responses in a CPI, or by simply suppressing the sidelobes produced by each waveform/filter. Sidelobe coherence can be enhanced by adjusting the tunable PARC parameters; by reducing h or m , or increasing T_s [8], [11]. However, these strategies do adversely affect communication performance by increasing BER and/or decreasing the data rate. Alternatively, sidelobes can be suppressed via waveform-specific mismatched filtering [23]. Consequently, PARC can facilitate coding diversity REC with high data rates and a minimal impact on radar performance.

From a spectrum sharing perspective it is clearly desirable to constrain each PARC waveform to the same spectral footprint as the base radar waveform. However, the phase-addition in (1) would naturally cause the spectrum to broaden. For chirp-like waveforms (e.g. LFM and most non-linear FM) this spectral broadening can be avoided by using “null” guard symbols at the beginning and end of each pulse [11]. These guard symbols translate into guard bands at the edges of the waveform spectrum, thereby eliminating spectral broadening.

Given knowledge of the base radar waveform, communication system parameters, and channel equalization and synchronization capability, demodulation at the communication receiver can be performed by first multiplying the incident signal by $\exp \{-j\psi(t; \bar{\beta})\}$, which realizes

$$\begin{aligned} r(t; \alpha, h, T_s) &= \exp \{ -j\psi(t; \bar{\beta}) \} \left(\sqrt{P_{\text{RX}}} s(t; \bar{\beta}, \alpha, h, T_s) + n(t) \right) \\ &= \sqrt{P_{\text{RX}}} \exp \{ j\phi(t; \alpha, h, T_s) \} + \hat{n}(t). \quad (2) \end{aligned}$$

Here P_{RX} is the incident power at the receiver, $n(t)$ is a white complex-valued Gaussian noise process, and $\hat{n}(t) = \exp \{-j\psi(t; \bar{\beta})\} n(t)$ is the resulting noise process, which is statistically equivalent to $n(t)$. For a communication receiver located at azimuth angle θ_0 and distance R , and a radar transmitter with peak power P_{TX} , the power at the communication receiver is

$$P_{\text{RX}} = \underbrace{\left(\frac{\lambda^2 G_{\text{RX}} P_{\text{TX}}}{16\pi^2} \right)}_{\mu} \frac{G_{\text{TX}}(\theta_0)}{R^2}, \quad (3)$$

where λ is free-space wavelength, G_{RX} is the receive antenna power gain, and $G_{\text{TX}}(\theta_0)$ is the transmit antenna power gain for azimuth angle θ_0 . If all communication receivers are equipped with identical components the terms in (3) aside from the transmit gain and distance can be grouped into the constant μ .

The symbol error rate (SER) of full-response CPM with a rectangular shaping filter can be approximated as [24]

$$\text{SER}(h, T_s, m, P_{\text{TX}}, \theta_0, R, N_0) \approx D_m Q \left(\sqrt{2\mu \frac{T_s G_{\text{TX}}(\theta_0) P_{\text{TX}}}{R^2 N_0} \left(1 - \frac{\sin(2h\pi)}{2h\pi} \right)} \right), \quad (4)$$

where $1 \leq D_m < 2$ is some constant depending on the modulation order m and $Q(x) = \int_x^\infty \frac{1}{\sqrt{2\pi}} \exp\{-t^2/2\} dt$. For the binary case the BER is equal to the SER, while for higher order modulations it is bounded as $\text{SER}/m < \text{BER} < \text{SER}$. We refer to the argument of the square root inside the Q function as the *effective communication SNR*.

III. FAR-FIELD RADIATED EMISSION DESIGN

The other form of waveform diversity considered here is spatial diversity, where dual-functionality is enabled by simultaneously transmitting radar and communication signals in distinct spatial directions from an antenna array. As with coding diversity it is desired for the radar and communication signals to have the same spectral and temporal support. One such approach is FFRED [12], which formulates a physical waveform design problem within a MIMO arrangement.

Consider a uniform linear array with N elements and an inter-element spacing of d . With FFRED the waveforms emitted concurrently by the N elements in each PRI are designed such that they combine in the far field to realize a desired radar signal in azimuth direction θ_r and a desired communication signal² in azimuth direction θ_c . Due to one-way path loss, the power requirement for the communication function is much lower than that for the radar function. As such, the power emitted in direction θ_c can be much less than that emitted in direction θ_r . It follows that, since the pulse-to-pulse variation of the communication component lies outside the radar mainbeam, the intra-CPI variation in clutter returns, and hence the severity of RSM, is limited. Because the FFRED approach restricts the radar and communication signals to occupy the same spectral and temporal support, the FFRED data rate (in bits/s) is on the order of the time-bandwidth product times the PRF, i.e. the same as PARC.

The FFRED emission constraints can be expressed by

$$\begin{aligned} \sum_{n=0}^{N-1} x_n(t) \exp \left\{ jn \frac{2\pi}{\lambda} d \sin \theta_r \right\} &= s_r(t) \\ \sum_{n=0}^{N-1} x_n(t) \exp \left\{ jn \frac{2\pi}{\lambda} d \sin \theta_c \right\} &= s_c(t), \end{aligned} \quad (5)$$

where $s_r(t)$ and $s_c(t)$ are the desired far-field radar and communication signals, respectively, and $x_n(t)$ is the waveform emitted by the n -th antenna element for $n = 0, 1, \dots, N-1$. It is important to note that by imposing the emission constraints in (5), FFRED also realizes a relative power allocation between

the radar and communication directions. The desired signals and the N emitted waveforms are discretized into the length- KN_{ov} vectors \mathbf{s}_r , \mathbf{s}_c , and \mathbf{x}_n , $n = 0, \dots, N-1$, where N_{ov} is the oversampling factor relative to 3-dB bandwidth, which is chosen to achieve sufficient fidelity for physical waveform realizations (provides the necessary spectral containment). Then the emission constraints can be rewritten as

$$\begin{aligned} \mathbf{v}^H(\theta_r) \mathbf{X} &= \mathbf{s}_r^T \\ \mathbf{v}^H(\theta_c) \mathbf{X} &= \mathbf{s}_c^T, \end{aligned} \quad (6)$$

where $\mathbf{X} = [\mathbf{x}_0 \mathbf{x}_1 \dots \mathbf{x}_{N-1}]^T$ is the $N \times KN_{\text{ov}}$ matrix that has the N discretized waveforms as its rows, and $\mathbf{v}(\theta_r)$ and $\mathbf{v}(\theta_c)$ are spatial steering vectors, defined for an arbitrary θ as

$$\mathbf{v}(\theta) = \left[1 \exp \left\{ -j \frac{2\pi}{\lambda} d \sin \theta \right\} \dots \exp \left\{ -j(N-1) \frac{2\pi}{\lambda} d \sin \theta \right\} \right]^T. \quad (7)$$

The FFRED formulation then determines the set of N MIMO waveforms by solving the optimization problem

$$\begin{aligned} &\text{minimize } \|\mathbf{X}\|_F^2 \\ &\text{subject to } \mathbf{V}^H(\theta_r, \theta_c) \mathbf{X} = \mathbf{S} \\ &|\mathbf{X}(k, i)| = |\mathbf{X}(l, j)| \text{ for } k, l = 0, \dots, N-1 \\ & \quad \quad \quad i, j = 0, \dots, KN_{\text{ov}} - 1, \end{aligned} \quad (8)$$

where $\|\mathbf{X}\|_F^2$ is the squared-Frobenius norm of \mathbf{X} , the matrix $\mathbf{V}(\theta_r, \theta_c) = [\mathbf{v}(\theta_r) \mathbf{v}(\theta_c)]$, and $\mathbf{S} = [\mathbf{s}_r \mathbf{s}_c]^T$.

In the absence of a constant-modulus constraint, (8) reduces to a minimum-norm problem, which is convex and has the closed-form solution

$$\mathbf{X}_* = \mathbf{V}(\theta_r, \theta_c) (\mathbf{V}(\theta_r, \theta_c)^H \mathbf{V}(\theta_r, \theta_c))^{-1} \mathbf{S}. \quad (9)$$

The minimum-norm solution \mathbf{X}_* has the smallest energy (i.e. Frobenius norm) of all waveform matrices satisfying the emission constraints. When a waveform constant-modulus is enforced the optimal solution can then be written as the sum of two waveform matrices, one corresponding to the subspace spanned by the columns of $\mathbf{V}(\theta_r, \theta_c)$ which is denoted as $\text{Col}[\mathbf{V}(\theta_r, \theta_c)]$ (i.e. \mathbf{X}_*), and the other as the orthogonal complement of $\text{Col}[\mathbf{V}(\theta_r, \theta_c)]$ denoted as \mathbf{X}_\perp^H . Thus

$$\tilde{\mathbf{X}} = \mathbf{X}_* + \mathbf{X}_\perp \quad (10)$$

where $\mathbf{V}^H(\theta_r, \theta_c) \mathbf{X}_\perp = \mathbf{0}$. Since $\mathbf{X}_* \mathbf{X}_\perp^H = \mathbf{0}$ as well due to their orthogonal complement relationship, the total energy $\|\tilde{\mathbf{X}}\|_F^2$ is the sum of the energies $\|\mathbf{X}_\perp\|_F^2$ and $\|\mathbf{X}_*\|_F^2$. In fact, the constant-modulus constraint can only be satisfied when $\|\mathbf{X}_\perp\|_F^2 \neq 0$.

In light of the solution in (10) a two-stage iterative optimization method was developed in [12]. This approach was shown to be effective at finding a feasible solution with unity PAPR via simulations [12] and demonstrated experimentally in [20]. However, the requisite computational complexity may be prohibitive in some operating scenarios. More importantly, due to the oversampling (relative to 3-dB bandwidth) necessary to ensure spectral containment of the desired radar/communication

²For simplicity we only consider a single communication signal, though FFRED could be employed to generate as many as $N-2$.

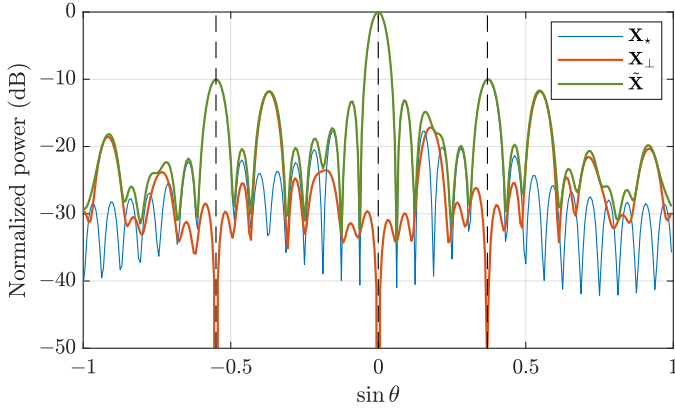


Fig. 1. Average beam patterns of the complete FFRED+PARC optimized emission (green), minimum-norm emission (blue), and orthogonal complement emission (red) for $L = 3$ desired signals with $h_0 = h_1 = h_2 = \frac{1}{8}$ and non-radar power levels $\gamma_1 = \gamma_2 = -10$ (dB).

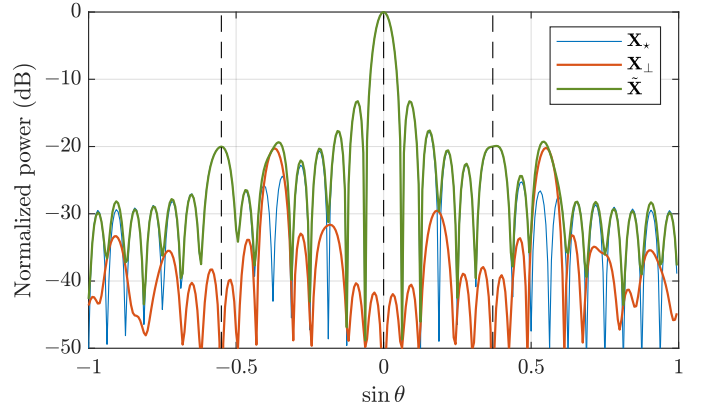


Fig. 2. Average beam patterns of the complete FFRED+PARC optimized emission (green), minimum-norm emission (blue), and orthogonal complement emission (red) for $L = 3$ desired signals with $h_0 = h_1 = h_2 = \frac{1}{8}$ and non-radar power levels $\gamma_1 = \gamma_2 = -20$ (dB).

signals, some undesired spectral spreading has been observed for other spatial directions.

In [25] the FFRED problem was reformulated in a general setting for an arbitrary antenna array geometry to generate $L \leq N - 1$ arbitrary desired signals in L spatial directions. A relaxed optimization problem was posed that significantly reduces computational complexity while achieving near-optimal performance when initialized with the minimum-norm solution. Nevertheless, like the approach in [12], this new FFRED approach still suffers from spectral spreading. Further, communication transmission was still only considered in the sidelobe region.

IV. FFRED + PARC

We now consider how the FFRED and PARC formulations can be combined as a means to offset their respective limitations. Communication data can be embedded into the radar mainbeam while controlling the severity of RSM via the tunable PARC parameters [11] or adaptive receiver processing [23], [26]. Moreover, it will be shown that the spectral spreading inherent in FFRED can be reduced by invoking a common base radar waveform in all desired signals and by using PARC guard symbols.

The most general approach to combine the PARC and FFRED approaches is to define each of the L desired signals (in directions θ_ℓ) as a PARC waveform with independent parameters $\beta_\ell, h_\ell, m_\ell, T_s^{(\ell)}$ carrying communication sequence α_ℓ , for $\ell = 0, \dots, L-1$. All waveforms have duration T and time-bandwidth product K (i.e. the same bandwidth). Without loss of generality, signal index $\ell = 0$ denotes the direction of the radar mainbeam. We define the desired power levels in the remaining spatial directions $\theta_\ell, \ell = 1, \dots, L-1$, relative to the power emitted in the direction θ_0 via

$$\gamma_\ell = \frac{G_{\text{TX}}(\theta_\ell)}{G_{\text{TX}}(\theta_0)}, \quad (11)$$

where $G_{\text{TX}}(\theta_\ell)$ is the transmit power gain achieved by the far-field combining of FFRED waveforms in spatial direction

θ_ℓ . The FFRED emission constraints of (5) can therefore be expressed as

$$\sum_{n=0}^{N-1} x_n(t) \exp \left\{ jn \frac{2\pi}{\lambda} d \sin \theta_\ell \right\} = \sqrt{\gamma_\ell} \exp \left\{ j \left(\psi_\ell(t; \bar{\beta}_\ell) + \phi_\ell(t; \alpha_\ell, h_\ell, T_s^{(\ell)}) \right) \right\}, \quad (12)$$

for $\ell = 0, \dots, L-1$ and with $\gamma_0 = 1$. With this configuration, for large N , the theoretical data throughput is on the order $N \times K \times \text{PRF}$ (bits/s).

While there are a variety of permutations of this general framework, here we consider the case in which all desired signals share a common base radar waveform, i.e. $\bar{\beta}_\ell = \bar{\beta}$ for all $\ell = 0, \dots, L-1$ in (12). The objective of this arrangement is to introduce correlation among the far-field desired signals as a means to achieve better spectral containment across all spatial angles. This combination of FFRED and PARC can improve spatial coverage while limiting the impact that the added mainbeam communication functionality has on radar performance. In addition, the structured coherence among the desired signals reduces the spectral spreading inherent in the original FFRED formulation [12], [25]. We refer to the combination as FFRED+PARC waveform design.

V. NUMERICAL RESULTS

Consider a uniform linear array of $N = 32$ elements with half-wavelength spacing. This array emits $L = 3$ desired signals, each with a time-bandwidth product of $K = 128$ and oversampled by a factor of $N_{\text{ov}} = 4$. The base radar waveform for all 3 desired signals is an up-chirp LFM. For FFRED waveform optimization the near-optimal approach from [25] is used. All communication sequences are binary with $N_s = 128$ bits/pulse (for a total data rate of 384 bits/pulse).

Figures 1 and 2 show the average beam patterns realized with FFRED+PARC, where averaging is performed in time for each pulse (i.e. the aggregate response over the pulsewidth) and across a large number of pulses with independent communication data. The spatial directions of the different beams

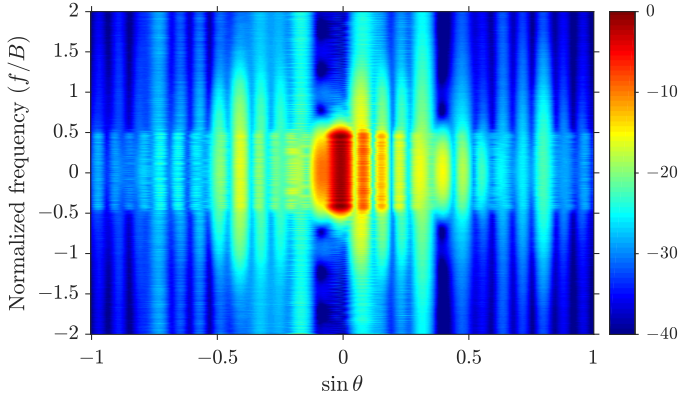


Fig. 3. The space-frequency power density for $L = 3$ FFRED signals: an LFM signal in the main beam, and two CPM communication signals (without a base radar waveform) and with $h_1 = h_2 = \frac{1}{2}$ and relative power levels $\gamma_1 = -10$ (dB) and $\gamma_2 = -16$ (dB).

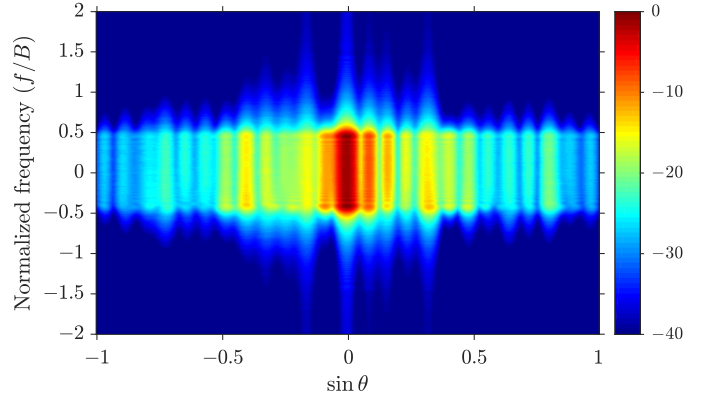


Fig. 6. The space-frequency power density for $L = 3$ FFRED+PARC signals, with $h_0 = h_1 = h_2 = \frac{1}{16}$ and power levels $\gamma_1 = -10$ (dB) and $\gamma_2 = -16$ (dB).

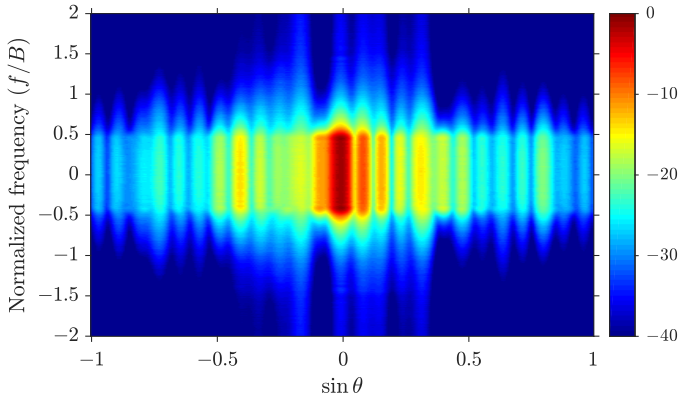


Fig. 4. The space-frequency power density for $L = 3$ FFRED+PARC signals, with $h_0 = h_1 = h_2 = \frac{1}{8}$ and power levels $\gamma_1 = -10$ (dB) and $\gamma_2 = -16$ (dB).

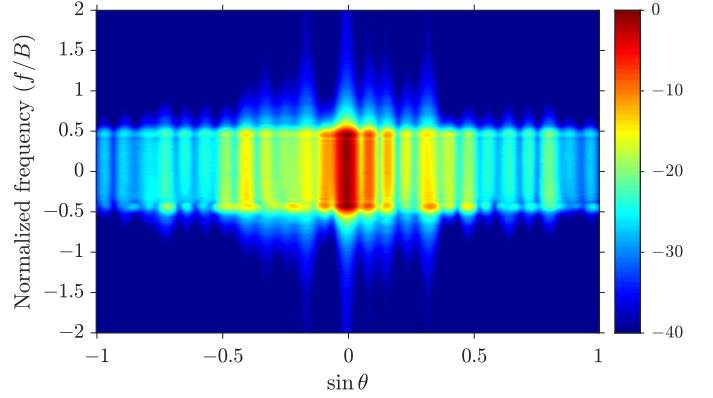


Fig. 7. The space-frequency power density for $L = 3$ FFRED+PARC signals, with $h_0 = h_1 = h_2 = \frac{1}{16}$, 16 guard symbols each, and power levels $\gamma_1 = -10$ (dB) and $\gamma_2 = -16$ (dB).

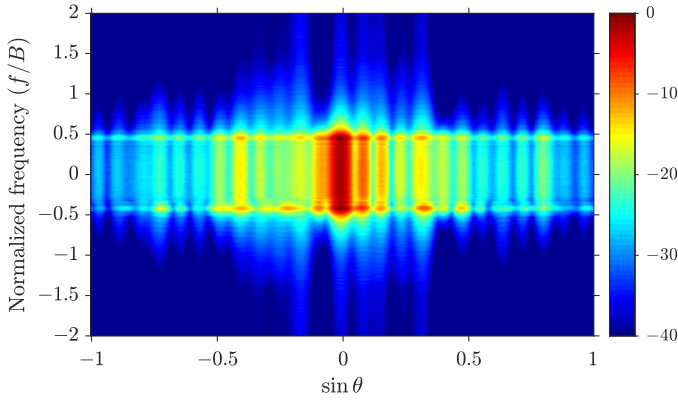


Fig. 5. The space-frequency power density for $L = 3$ FFRED+PARC signals, with $h_0 = h_1 = h_2 = \frac{1}{8}$, 32 guard symbols each, and power levels $\gamma_1 = -10$ (dB) and $\gamma_2 = -16$ (dB).

are $\sin \theta_0 = 0$, $\sin \theta_1 = -0.55$, and $\sin \theta_2 = +0.37$, with a common modulation index of $h_0 = h_1 = h_2 = \frac{1}{8}$. The relative power levels of the non-radar beams γ_1 and γ_2 are set to -10 dB in Fig. 1 and -20 dB in Fig. 2. In each figure the beampatterns of the minimum-norm solution \mathbf{X}_* (blue), the orthogonal complement component \mathbf{X}_\perp (red), and the

complete FFRED+PARC solution $\tilde{\mathbf{X}} = \mathbf{X}_* + \mathbf{X}_\perp$ (green) are shown. For both figures the PAPR of $\tilde{\mathbf{X}}$ was verified to be 1. Likewise the time-domain structure of the desired signals were confirmed to be realized in their respective intended directions. It is observed in both figures that the orthogonal complement component has nulls in those intended directions. We also observe additional (unintended) beams that are caused by the energy in the orthogonal complement. The power of these nuisance beams and the sidelobe level in each beampattern rises with the power level in the beams $l = 1$ and 2.

Figures 3–7 show space-frequency power density plots as a function of the modulation index h and the number of guard symbols. The intended signal directions are $\sin \theta_0 = 0$, $\sin \theta_1 = +0.4$, and $\sin \theta_2 = -0.08$, with relative power levels $\gamma_1 = -10$ dB and $\gamma_2 = -16$ dB. To quantify the spectral spreading in each case we define the percent out-of-band spectral content as a metric relative to 3-dB bandwidth of the base radar waveform. The percent out-of-band spectral content is computed from the aggregate spectrum obtained by integrating across all spatial directions.

In Fig. 3 signals $\ell = 1$ and 2 carry data, with $h_1 = h_2 = \frac{1}{2}$, which translates to a data rate of 256 bits/pulse. In Figures 4 and 6 all three signals carry data (for a data rate

of 384 bits/pulse) with $h_0 = h_1 = h_2 = \frac{1}{8}$ in Fig. 4 and $h_0 = h_1 = h_2 = \frac{1}{16}$ in Fig. 6. In Fig. 5 all parameter values are the same as those in Fig. 4, with the exception of 32 total guard symbols (16 at each end of the pulse, for a data rate of 288 bits/pulse). Likewise, in Fig. 7, all parameters are the same as those in Fig. 6 with the exception of 16 total guard symbols (8 at each end of the pulse, for a data rate of 336 bits/pulse).

We observe that the spectral spreading is reduced in Fig. 4 compared to Fig. 3, and further reduced in Fig. 5 where guard symbols are used. Likewise, the spectral spreading is even further reduced in Figures 6 and 7 compared to Figures 4 and 5, respectively, with Fig. 7 providing the most compact spectrum.

The percent out-of-band spectral content for Figures 3–7 are 14.57%, 7.11%, 4.84%, 4.19% and 3.62%, respectively. For reference, the percent out-of-band spectral content of just an LFM base radar waveform is computed as 2.12%. As anticipated the spectral spreading is significantly mitigated with the FFRED+PARC framework. However, we emphasize that there is a trade-off between the communication performance (i.e. BER and data rate) and the spectral spreading. In particular, the use of guard symbols reduces the data rate, while reducing the modulation index h decreases the effective communication SNR and therefore increases BER.

VI. CONCLUSIONS AND FUTURE WORK

We have introduced a MIMO based dual-function waveform design approach denoted as FFRED+PARC that leverages the benefits of these individual methods to perform joint radar/communications. This combined approach is capable of transmitting independent data streams in multiple spatial directions (up to the number of antenna elements) simultaneously, including in the radar mainbeam, achieving a rate on the order of the time-bandwidth product times the PRF per stream. In addition, the resultant waveforms are power efficient and spectrally well-contained. The effectiveness of the FFRED+PARC framework on spectral containment was demonstrated by numerical results in simulation, with experimental demonstration planned for the near future.

The impact of the added mainbeam communication capability on radar performance can be controlled via the tunable PARC parameters. Nevertheless, future work includes the evaluation and analysis of the RSM effect within this FFRED+PARC framework.

REFERENCES

- [1] H. Griffiths, L. Cohen, S. Watts, E. Mokole, C. Baker, M. Wicks, and S. D. Blunt, "Radar spectrum engineering and management: technical and regulatory issues," *Proceedings of the IEEE*, vol. 103, no. 1, pp. 85–102, Jan. 2015.
- [2] S. D. Blunt and E. S. Perrins, Eds., *Radar & Communication Spectrum Sharing*. London, UK: IET, 2018.
- [3] B. Paul, A. R. Chiriyath, and D. W. Bliss, "Survey of RF communications and sensing convergence research," *IEEE Access*, vol. 5, pp. 252–270, Dec. 2017.
- [4] R. A. Romero and K. D. Shepherd, "Friendly spectrally shaped radar waveform with legacy communication systems for shared access and spectrum management," *IEEE Access*, vol. 3, pp. 1541–1554, Aug. 2015.
- [5] J. G. Metcalf, C. Sahin, S. D. Blunt, and M. Rangaswamy, "Analysis of symbol-design strategies for intrapulse radar-embedded communications," *IEEE Transactions on Aerospace and Electronic Systems*, vol. 51, no. 4, pp. 2914–2931, Oct. 2015.
- [6] A. Hassaniien, C. Sahin, J. G. Metcalf, and B. Himed, "Uplink signaling and receive beamforming for dual-function radar communications," *IEEE International Workshop On Signal Processing Advances in Wireless Communications*, Kalamata, Greece, June 2018.
- [7] M. P. Daly and J. T. Bernhard, "Directional modulation technique for phased arrays," *IEEE Transactions on Antennas and Propagation*, vol. 57, no. 9, pp. 2633–2640, Sep. 2009.
- [8] S. D. Blunt, M. R. Cook, and J. Stiles, "Embedding information into radar emissions via waveform implementation," *International Waveform Diversity and Design Conference*, pp. 195–199, Niagara Falls, Canada, Aug. 2010.
- [9] M. Nowak, M. Wicks, Z. Zhang, and Z. Wu, "Co-designed radar-communication using linear frequency modulation waveform," *IEEE Aerospace and Electronic Systems Magazine*, vol. 31, no. 10, pp. 28–35, Oct. 2016.
- [10] A. Hassaniien, M. G. Amin, Y. D. Zhang, and F. Ahmad, "Dual-function radar-communications: information embedding using sidelobe control and waveform diversity," *IEEE Transactions on Signal Processing*, vol. 64, no. 8, pp. 2168–2181, Apr. 2016.
- [11] C. Sahin, J. Jakobosky, P. M. McCormick, J. G. Metcalf, and S. D. Blunt, "A novel approach for embedding communication symbols into physical radar waveforms," *IEEE Radar Conference*, pp. 1498–1503, Seattle, WA, May 2017.
- [12] P. M. McCormick, S. D. Blunt, and J. G. Metcalf, "Simultaneous radar and communication emissions from a common aperture, part I: theory," *IEEE Radar Conference*, Seattle, WA, May 2017.
- [13] N. A. O'Donoghue, "Analysis of dual-transmit beams," *IEEE Radar Conference*, pp. 1233–1238, Seattle, WA, May 2017.
- [14] B. Ravenscroft, P. M. McCormick, S. D. Blunt, E. Perrins, and J. G. Metcalf, "A power-efficient formulation of tandem-hopped radar & communications," *IEEE Radar Conference*, Oklahoma City, OK Apr. 2018.
- [15] C. Sahin, P. M. McCormick, and B. Ravenscroft, "Embedding communications into radar emissions by transmit waveform diversity," in *Radar & Communication Spectrum Sharing*, S. D. Blunt and E. S. Perrins, Eds. IET, 2018.
- [16] P. M. McCormick, C. Sahin, S. D. Blunt, and J. G. Metcalf, "FMCW implementation of phase-attached radar-communications (PARC)," *IEEE Radar Conference*, Boston, MA, April 2019.
- [17] S. D. Blunt and E. L. Mokole, "Overview of radar waveform diversity," *IEEE Aerospace and Electronic Systems Magazine*, vol. 31, no. 11, pp. 2–42, Nov. 2016.
- [18] G. C. Tavik, C. L. Hilterbrick, J. B. Evins, J. J. Alter, J. G. Crnkovich, J. W. de Graaf, W. Habicht, G. P. Hrin, S. A. Lessin, D. C. Wu, and S. M. Hagewood, "The advanced multifunction RF concept," vol. 53, no. 3, pp. 1009–1020, March 2005.
- [19] C. Sahin, J. G. Metcalf, and S. D. Blunt, "Characterization of range sidelobe modulation arising from radar embedded-communications," *IET International Conference on Radar Systems*, Belfast, UK, Oct. 2017.
- [20] P. M. McCormick, S. D. Blunt, and J. G. Metcalf, "Simultaneous radar and communication emissions from a common aperture, part II: experimentation," *IEEE Radar Conference*, Seattle, WA, May 2017.
- [21] S. D. Blunt, M. R. Cook, J. Jakobosky, J. De Graaf, and E. Perrins, "Polyphase-coded FM (PCFM) radar waveforms, part i: implementation," *IEEE Transactions on Aerospace and Electronic Systems*, vol. 50, no. 3, pp. 2218–2229, July 2014.
- [22] J. B. Anderson, T. Aulin, and C.-E. Sundberg, *Digital Phase Modulation*. New York, NY: Plenum Press, 1986.
- [23] C. Sahin, J. G. Metcalf, and S. D. Blunt, "Filter design to address range sidelobe modulation in transmit-encoded radar-embedded communications," *IEEE Radar Conference*, pp. 1509–1514, Seattle, WA, May 2017.
- [24] J. G. Proakis, *Digital Communications*. New York, NY: McGraw-Hill Education, 2008.
- [25] P. M. McCormick, C. Sahin, S. D. Blunt, and J. G. Metcalf, "Physical waveform optimization for multiple-beam multifunction digital arrays," *Asilomar Conference on Signals, Systems, and Computers*, Pacific Grove, CA, Oct. 2018.
- [26] C. Sahin, J. G. Metcalf, and B. Himed, "Reduced complexity maximum SINR receiver processing for transmit-encoded radar-embedded communications," *IEEE Radar Conference*, Oklahoma City, OK, Apr. 2018.